Stimulation of microbially-mediated chromate reduction in alkaline soil-water systems

D.I. Stewart
School of Civil Engineering, University of Leeds, Leeds LS2 9JT, UK
Corresponding Author: E-mail: d.i.stewart@leeds.ac.uk

I.T. Burke and R.J.G. Mortimer
School of Earth and Environment, University of Leeds, Leeds LS2 9JT, UK

Abstract

Acetate was added to two closed soil-water systems that are representative of the subsurface environment close to chromium ore processing residue disposal sites; one had a pH of 7.7, the other 9.3. Cr(VI) reduction occurred in both systems as part of a cascade of microbially mediated terminal electron accepting processes, occurring between nitrate and iron reduction. Cr(VI) and subsequently iron reduction took longer to start and were slower in the more alkaline system. At the point when Cr(VI) reduction was essentially complete, the microbial populations in both systems showed a significant increase in species closely related to β-proteobacteria that are capable of nitrate reduction.

BACKGROUND

Poorly controlled landfilling of chromite ore processing residue (COPR), particularly highly alkaline COPR from the high-lime process, is a globally widespread problem (Geelhoed et al. 2002). Chromite ore is processed by roasting it with an alkali-carbonate at 1150°C to oxidise the insoluble Cr(III) to soluble Cr(VI) which is then extracted with water upon cooling. Traditionally, limestone was added to the reaction mixture to improve air penetration, and this "high-lime" process was the only commercial method of chromium smelting in the UK up to the 1960s (Darrie 2001). In that time vast quantities of COPR were produced, and many millions of tonnes have been deposited in and around urban areas (e.g.

Glasgow, Bolton (Breeze 1973; Geelhoed et al. 2002)). Additionally, the high lime process is still generating chromium contaminated wastes in countries such as China, Russia, India and Pakistan (a total of 600,000 $t.yr^{-1}$ in 2001; Darrie 2001).

COPR from the high-lime process and typically contains 2-6% total chromium by weight (Deakin et al. 2001; Geelhoed et al. 2002; Gemmell 1973). Much of the chromium in COPR is unreacted insoluble chromite ore (i.e. Cr(III)) but, as a result of oxidation during ore processing, up to 30% can be chromate (Cr(VI)) (Geelhoed et al. 2003). As a result, the pore water in abandoned waste piles can contain up to ca. 640 $\mu mol.l^{-1}$ of chromate (Deakin 2002; Farmer et al. 1999). This is problematic because the chromate anion (CrO_4^{2-}) is very mobile in groundwater systems, whereas Cr(III) is generally strongly retained by soil via sorption and precipitation as chromium(III) hydroxide (Fendorf 1995; Guertin et al. 2005; Lloyd and Macaskie 1996; Lovley 1993; Richard and Bourg 1991; Viamajala et al. 2002b). Cr(VI) is carcinogenic, mutagenic and toxic, whereas Cr(III) is an essential micronutrient for plant and animal metabolism (Fendorf 1995; Geelhoed et al. 2003; Richard and Bourg 1991).

Addition of a suitable organic substrate to a groundwater system stimulates growth in the indigenous microbial population and rapidly depletes the dissolved oxygen (Scherer et al. 2000). Typically, as microbial anoxia develops a cascade of reducing reactions then occur due to increased activity of indigenous microbes (Burke et al. 2005) that can conserve the free energy yield from coupling reduction processes to the oxidation of organic matter. Microbial processes releasing most energy are favoured, so the sequence observed typically follows the decreasing order of redox potentials shown in Table 1 (calculated from standard thermodynamic data using the Nernst equation). Thus dramatic increases in the numbers of

nitrate-, metal- and sulphate-reducing bacteria usually develop in sequence (Anderson et al. 2003; Holmes et al. 2002).

There is an extensive body of research on microbially mediated chromate reduction, both in pure microbial cultures (e.g. Daulton et al. 2007; Viamajala et al. 2002a; e.g. Viamajala et al. 2002b; Viamajala et al. 2004) and in environmental samples (e.g. Bader et al. 1999; Donmez and Kocberber 2005; Fude et al. 1994; Moser et al. 2003; Schmieman et al. 2000). This literature suggests that microbially mediated reduction of contaminant metal ions is often a secondary reaction of a microorganism respiring with another electron acceptor (Chen and Hao 1998; Fude et al. 1994; Holmes et al. 2002). Reduction can be either the result of enzymatic reactions within the cell or cell wall (Chen and Hao 1998; Daulton et al. 2007), or the result from an extracellular reaction with reduced species produced by respiration (Lloyd et al. 1998). Cr(VI) can readily cross cell membranes by the sulphate transport system (Cervantes et al. 2001), where anaerobic enzymatic reduction to Cr(III) appears to proceed via unstable Cr(V) and Cr(IV) intermediates (Neal et al. 2002; Suzuki et al. 1992), with evidence that the terminal microbial reduction step produces Cr(II) (Daulton et al. 2007); once expelled from the cell the Cr(II) oxidizes to the more stable trivalent state. Equally, though, Cr(VI) is readily reduced to Cr(III) by species such as Fe(II) and S^{2-} produced by anaerobic cell respiration (Richard and Bourg 1991).

Nearly all the reported work on microbially mediated Cr(VI) reduction has been conducted at near neutral pH, and much less is generally known about metal reduction in the alkaline environments that will be representative of COPR disposal sites (Ye et al. 2004). This paper reports a comparative study into microbially mediated chromate reduction in circum-neutral and more alkaline soil-water systems representative of those around the margins of COPR

disposal sites. It reports geochemical changes that occur as microbially induced anoxia develops in closed systems, changes in the microbial population that develop concurrently, and highlights differences between the circum-neutral and alkaline systems.

METHODOLOGY

Sampling Site Description. The site (Figure 1) covers an area of around 8 hectares (80,000 m^2) in the north west of England (Breeze 1973; Gemmell 1973). Some 800,000 m^3 of COPR produced between 1893 and 1966 is deposited at the site. Site restoration was undertaken in the late 1960's, when the waste was capped with gravel (20 cm) as a capillary break, and topsoil (15 cm) to provide a rooting medium (Breeze 1973). The site was landscaped to direct infiltration into a drainage system at the site margins. The site is now covered with grass, and has trees around its margins. However, some grassed areas show signs of distress and there are frequent leachate over- flow incidents due to precipitates blocking the drainage system. The pore water in COPR has elevated sulphate, calcium and sodium concentrations, high pH and can contain ca. 600 $\mu mol.l^{-1}$ of chromate (see table 2).

Soil Sampling and Characterisation. Samples from topsoil and subsoil horizons were taken at two locations (sample H4 was taken on 4th April, 2006 from location 1 and sample FL9 was taken on 8th May, 2006 from location 2). These were within 20m down slope from the edge of the COPR waste material (see site plan, Figure 1). Both locations were visibly affected by periodic influxes of high pH COPR waste leachate (both were immediately down-slope of areas where precipitate formation marked the emergence of leachate from the waste). Several samples taken from each location but only one sample from each area was used in the experiments reported here. Sample H4 came from a depth of 50 cm under sparse grass cover and had a water content of 24%, whereas sample FL9 came from a depth of 10 cm in scrub

woodland (the soil cover was very thin) and had a water content of 22%. A spade was used to reach the required depth before the soils were sampled into clean polythene containers using a clean steel spatula (washed in 70% ethanol/water prior to use). Soils were transported back to the laboratory within 2 hours of sampling and stored at 4°C until use. Experiments were started within one month of collecting the second sample and soil manipulation was kept to a minimum prior to incubation. In addition, following the protocol of Burke et al. (2005) brook water was taken from a location unaffected by either COPR waste or site leachates as close as possible upstream from location 1 (Figure 1) for creating soil microcosms.

X-ray diffraction (XRD) analysis of soil samples ground to <75μm was undertaken on a Philips PW1050 Goniometer, and x-ray fluorescence (XRF) analysis of fused soil samples was undertaken on an ARL 9400 wavelength dispersive sequential spectrometer. These analyses indicated that the dominant crystalline phase in H4 is quartz with some feldspar. The dominant mineral phase in FL9 is also quartz, but with some calcite and small amounts of haematite and feldspar. The loss on ignition was 6% and 14% for the two samples, respectively, representing organic matter, bound water and, in the case of the second sample, CO_2 lost from calcite. H4 contained 1.8 $g.kg^{-1}$ of chromium and FL9 contained 1.4 $g.kg^{-1}$. A leaching test was conducted on each soil where 10g of each soil was shaken with 100 ml of deionised water and allowed to equilibrate for 48 hours. The aqueous sulphate concentrations in the leaching tests on H4 and FL9 (determined by ion chromatography on a Dionex ICS-90 with an AS14 analytical column) were 18 and 540 $\mu mol.l^{-1}$, respectively.

The water sample taken from the brook immediately upstream of the site in April 2006 had a pH of 7.3 and contained 133 $\mu mol.l^{-1}$ nitrate, 350 $\mu mol.l^{-1}$ sulphate (measured by ion chromatography), and 130 $mg.l^{-1}$ total dissolved salts. Total alkalinity, measured by titration

with HCl to pH 5 using bromocreosol green/methyl red indicator, was equivalent to 880 ± 70 $\mu mol.l^{-1}$ of $CaCO_3$.

Reduction Microcosm Experiments. Microcosms were made up using 10 g of soil and 100 ml of brook water in 120 ml glass serum bottles (Wheaton Scientific, NJ, USA) and sealed with butyl rubber stoppers (Bellco Glass Inc., NJ, USA) and aluminium crimps. Soil microcosms containing soil from H4 and FL9 when equilibrated with brook waters produced microcosm experiments at pH 7-8 and pH 9-10 respectively. For each pH system three repeat microcosms were amended to produce a final concentration of 250 $\mu mol.l^{-1}$ Cr(VI) (as potassium chromate) and 20 $mmol.l^{-1}$ sodium acetate (called the *active* microcosms). Cr(VI)- and acetate-amended sterile control microcosms were established by heat treatment for 20 minutes at 120°C (*sterile*). In addition unsterilised control microcosms containing only unamended soils and brook water (*unamended*), and unsterilised control microcosms containing 250 $\mu mol.l^{-1}$ Cr(VI) but no acetate addition (*chromate only*) were also established. All microcosm experiments and controls were incubated anaerobically at 25 ±2°C in the dark. Microcosm experiments and controls were periodically sub-sampled for geochemical and microbiological analysis over 72 days to produce a progressive anoxia time series. During sampling soil microcosms were shaken and 3 ml of soil slurry withdrawn using aseptic technique with sterile syringes and needles (Burke et al. 2006). Samples were centrifuged (5 min, 16,000g) and then pore water and soil were analysed for a range of redox indicators, Cr(VI) and microbiology (see below).

Geochemical Methods. Cr(VI) and total Fe were determined by standardised UV-vis spectroscopy methods on a Cecil CE 3021 (US-EPA 1992; Viollier et al. 2000) and sulfate and nitrate were determined by ion chromatography on a Dionex ICS-90 with AS14 analytical

column. Fe(II) in solids was determined after extraction by 0.5 N HCl and reaction with Ferrozine™ (Lovley and Phillips 1986). Standards were used regularly to check method quality and calibration linear regressions or quadratic fits normally produced r-squared values of 0.99 or better. Eh and pH readings were taken using Orion bench-top meters and calibrated electrodes.

Extraction of DNA from soil microbes. Microbial DNA was extracted from soil samples (0.25g) using a FastDNA spin kit and FastPREP instrument (Qbiogene, Inc.). DNA fragments in the size range 3 kb to ~20 kb were isolated on a 1% agarose "1x" Tris-borate-EDTA (TBE) gel stained with ethidium bromide for viewing under UV light (10x TBE solution supplied by Invitrogen Ltd., UK). The DNA was extracted from the gel using a QIAquick gel extraction kit from (QIAGEN Ltd, UK); final elution was by $1/10^{th}$ strength elution buffer (unless explicitly stated, the manufacturer's protocols supplied with all kits employed were followed precisely).

16S rRNA Gene Sequencing. A fragment of the 16S rRNA gene of approximately ~500 bp was amplified by Polymerase chain reaction (PCR) using broad-specificity bacterial primers in a Mastercycler gradient thermal cycler (Eppendorf, Germany). The DNA primers were 8f (5'-AGAGTTTGATCCTGGCTCAG-3') (Eden et al. 1991) and 519r (5'-GWATTACCGCGGCKGCTG-3') (Lane et al. 1985). Each PCR reaction mixture contained 25 µl of purified DNA, 5 units of either Taq DNA polymerase or GoTaq DNA polymerase (both from Promega Corp., USA), 1× PCR reaction buffer, 1.5mM $MgCl_2$ (already in the GoTaq reaction buffer), 0.2mM PCR nucleotide mix (Promega Corp., USA), and 0.6 µM DNA primers in a final volume of 50 µl. The reaction mixtures were incubated at 94°C for 4 min, and then cycled 30 times through three steps: denaturing (94°C, 30 s),

annealing (50°C, 30 s), primer extension (74°C, 60 s). This was followed by a final extension step at 74°C for 7min (the extension and final extension steps were conducted at 72°C when using GoTaq). The PCR products were purified using a QIAquick PCR Purification Kit (QIAGEN Ltd, UK). Amplification product sizes were verified by electrophoresis of 10 µl samples in a 1.0% agarose TBE gel with ethidium bromide straining.

The PCR product was ligated into a standard cloning vector (p-GEM-T Easy supplied by Promega), transformed into competent *E. coli* cells (JM109 competent cells or XL1-Blue supercompetent cells from Stratagene), and colonies were grown on LB- agar plates containing ampicillin (100 $\mu g.ml^{-1}$) surface dressed with IPTG and X-gal (as per the Stratagene protocol) for blue-white colour screening. Colonies containing the insert were re-streaked on LB-ampicillin agar plates, and single colonies from these plates were incubated overnight in liquid LB-ampicillin. Plasmid DNA was extracted using a QIAprep Spin minprep kit (QIAGEN Ltd, UK) and sent for automated DNA sequencing (ABI 3100*xl* Capilliary Sequencer) using the T7P primer. Sequences (typically ~520 bp) were analysed against the EMBL release nucleotide database in Sept 2007 using NCBI-BLAST2 program and matched to known 16S rRNA gene sequences. Default settings were used for the BLAST parameters (match/mismatch scores 2, -3, open gap penalty 5, gap extension penalty 2).

RESULTS

Reduction Microcosm Experiments. With the exception of the sterile control, the microcosms containing sample H4 had an initial pH of 7.7 ±0.1, and aqueous nitrate and sulphate concentrations of 137 ±8 and 360 ±36 $\mu mol.l^{-1}$ (see Figure 2), which are the same as the brook water concentrations. The H4 sterile control had an initial pH of 7.0, and aqueous nitrate and sulphate concentrations of 114 and 381 $\mu mol.l^{-1}$. The H4 active and chromate-only

microcosms had an aqueous Cr(VI) concentration of 255 ±8 μmol.l^{-1}. The sterile control and unamended microcosm had aqueous Cr(VI) concentrations of 225 and 0.5 μmol.l^{-1}, respectively.

In the microbially active microcosms containing sample H4 60% of the nitrate was removed from solution within 2 days and all the nitrate was removed in 4 days, whereas there was about a 15% increase in the nitrate in the three control tests. The aqueous chromate concentration in the active microcosms decreased by 22%, 63% and 90% in 2, 4, and 7 days, respectively, and was all removed by day 14. The aqueous chromate concentration in the sterile control decreased by about 12% over the first 36 days, but recovered to only 5% below its initial concentration after 72 days. The chromate-only control showed no significant change in the aqueous chromate concentration over 72 days, and the unamended control showed a small but steady increase in aqueous chromate concentration, reaching 19 μmol.l^{-1} on day 72. The sulphate concentration in the microbially active microcosms showed very little change during the first 21 days, reduced by 10% after 36 days and sulphate had completely gone by day 72. The sulphate concentration in the controls showed small, random variation without any significant change over 72 days. The average pH active microcosms typically fluctuated by ±0.2 pH units without any trend, but final pH was 0.4 higher than the initial average value. The pH of the controls fluctuated by up to 0.3 pH units without a significant overall change.

The percentage of the total 0.5 N HCl extractable iron present as Fe(II) was initially zero, but increased from 2% after 4 days to 91% after 21 days, increasing to 99% after 72 days. The percentage of 0.5 N HCl extractable iron present as Fe(II) in the control experiments was

initially zero, has a low values without a trend at later times, and at no time exceeds 5% in any control test.

The microcosms containing sample FL9 had an initial pH of 9.3 ±0.1 (see Figure 3). The control microcosms and active samples a and b had an aqueous nitrate concentration of 149 ±13 $\mu mol.l^{-1}$; active sample c had an aqueous nitrate concentration of 208 $\mu mol.l^{-1}$. The FL9 sterile control had a sulphate concentration of 1266 $\mu mol.l^{-1}$, but the remaining FL9 microcosms had a sulphate concentrations of 719 ±64 $\mu mol.l^{-1}$. The FL9 active and chromate-only microcosms had an aqueous chromate concentration of 260 ±4 $\mu mol.l^{-1}$. The sterile control and unamended microcosm had aqueous chromate concentrations of 230 and 12 $\mu mol.l^{-1}$, respectively.

In the active microcosms containing sample FL9 75% of the nitrate was removed from solution within 2 days and 98% was removed in 4 days, whereas there was little overall change in the nitrate in the three control tests (both the unamended and the chromate-only controls showed decrease at some intermediate time points but the final concentration was close to the initial concentration). The aqueous chromate concentration decreased significantly in all three microbially active experiments, but at differing rates. Averaging the divergent behaviour in these replicates (FL9a, b and c) could obscure the processes that are occurring, and therefore their behaviour is reported separately where appropriate. Chromate removal was most rapid in microcosm FL9b where aqueous concentration decreased by 11%, 88% and >99% in 7, 14, and 21 days, respectively. In microcosm FL9a the aqueous concentration decreased by 13%, 31% and 97% in 14, 21, and 36 days, respectively. Chromate removal was slowest in microcosm FL9c where aqueous concentration decreased by 14%, 59% and 92% in 14, 36, and 72 days, respectively. The aqueous chromate

concentration in the sterile control showed no significant change in the aqueous chromate concentration over 72 days, whereas that of the chromate-only control decreased by about 11% over 72 days. The aqueous chromate concentration of the unamended control increased over the test, reaching 25 $\mu mol.l^{-1}$ on day 72. The sulphate concentration showed the same increasing trend in all three active microcosms, roughly doubling in the first 7 days and nearly trebling over 72 days. The FL9 unamended and the chromate-only controls also showed a similar increasing trend, increasing by 250% and 160%, respectively, over 72 days, however the sulphate concentration of the sterile control remained relatively stable at its slightly higher initial value. The average pH of the active microcosms increased by 0.2 pH units over 72 days. The pH of the chromate only control was steady over the test period, whereas the pH of the sterile and unamended controls increased by 0.3 pH units.

The percentage of 0.5 N HCl extractable iron present as Fe(II) in the microbially active FL9 microcosms was initially about 13%. This proportion decreased during the first 4 days to about 5%, where it remained until day 14, when it increased at different rates in the three active microcosms. The proportion of total iron in the Fe(II) oxidation state increased most rapidly in microcosm FL9b where it was 13, 23 and 46% in 21, 36, and 72 days, respectively. In microcosm FL9a and FL9c it was 14%, 13% and 22%, and 11, 12 and 6% at the same time points. The percentage of total iron in the controls in the Fe(II) oxidation state varied between 0 and 6%, without a trend apparent, over the test period.

Microbiological Community Analysis. In order to evaluate potential changes in the microbial community associated with removal of Cr(VI) from solution in the neutral and alkaline microcosms, 16S rRNA gene sequences from the initial soils and of soil samples taken on day 14 of microcosm H4a and day 72 of microcosm FL9c were analyzed. These

times during the microcosm experiments were selected as the point when aqueous Cr(VI) removal from solution was substantially complete. Each 16S rRNA gene sequence has been assigned to a phylum (class in the case of proteobacteria) based >95% homology over a sequence length >400bp to a known sequence in the database (see figures 4 and 5). Full details of each 16S rRNA gene sequence for which an assignment has been made are reported in Appendix A.

From the initial H4 sample 42 clones were sequenced and 27 were assigned to a phylum. From the H4a-T_{14} sample 43 clones were sequenced and 37 were assigned to a phylum. The most significant changes over the first 14 days of microcosm H4a were an increase in the sequences closely related to β-proteobacteria, the appearance of sequences closely related to actinobacteria and δ-proteobacteria, a decrease in unidentified sequences, and a smaller decrease in sequences related to γ-proteobacteria.

Of the total number of clones from H4a-T_{14} that were sequenced, 9% were ≥97% homologous to Rhizobium species of α-proteobacteria (Rhizobium species are nitrogen fixing α-proteobacterium that often found existing symbiotically in plant roots; (Martinez-Romero 2003; Willems 2006), 19% of sequences were ≥95% homologous to a denitrifying Rhodocyclus specie of β-proteobacterium (AY691423; Smith et al. 2005), 7% of sequences were ≥99% homologous to nitrate reducing Comamanadaceae species of β-proteobacterium (either AJ505857 or AJ505848; Probian et al. 2003), and 9% of sequences were ≥97% homologous to Geobacteraceae specie of δ-proteobacterium (EF668930) found in Fe(III)-reducing subsurface environments.

From the initial FL9 sample 40 clones were sequenced and 21 were assigned to a phylum. From the FL9c-T_{72} sample 43 clones were sequenced and 36 were assigned to a phylum. The most significant change in microcosm FL9c was a large increase in the sequences from β-proteobacteria and a decrease in unidentified sequences. Of the total number of clones from FL9c-T_{72} that were sequenced, 63% of sequences were related to genera within the Comamonadaceae family of β-proteobacteria (≥96% identity), including 42% of the total number that were ≥99% homologous to Acidovorax species.

DISCUSSION

In the circum-neutral H4 microcosms, the three microbially active replicates responded similarly. Nitrate was rapidly removed shortly after the start of testing, iron reduction (from Fe(III) to Fe(II)) occurred next, sulphate removal followed on, and most of the sulphate had been removed from solution by day 72. This is only happened in the microbially active experiments, which demonstrates that these processes were microbially mediated and indicative of a cascade of terminal-electron-accepting processes developing in the normal sequence expected during the onset of progressive anoxia (Burke et al. 2005; NABIR 2003).

In the microbially active H4 experiments Cr(VI) removal from solution started sometime within the first two days, and was complete before day 14. Thus it started in a period when there was a significant rate of nitrate reduction, but continued after the aqueous nitrate had been exhausted. Cr(VI) removal was not observed in ether the sterile or chromate only controls, so is most likely to have been microbially mediated reduction of Cr(VI) to Cr(III). Cr(VI)-reduction occurs before Fe(III)-reduction is observed as an increase in % Fe(II) in the soil which suggests that Cr(VI) reduction may have been the result of direct enzymatic processes rather than an abiotic reaction with accumulated Fe(II). On day 14, when chromate

removal was essentially complete, a significant proportion of the microbial population appears to have been closely related to known nitrate reducing species. However four sequences were closely related to a Geobacteraceae specie of δ-proteobacteria. Such species are more usually associated with iron reducing environments (Lloyd and Macaskie 1996; Lovley et al. 1995). This may show that the total population may not be a guide to the active population. The latter sequences may be indicative of a switch to iron as the terminal electron acceptor.

In the alkaline FL9 microcosms the three active replicates responded at different rates, but followed a similar pattern of behaviour. Nitrate was rapidly removed near the start of the tests. A period followed in which the proportion of the total iron in the lower Fe(II) oxidation state is indistinguishable from the controls, and then period of iron reduction that in two of the active microcosms extended until the end of testing. This sequence of nitrate removal followed by iron reduction was only observed in the active microcosms indicating that was microbially mediated, and is strongly suggestive of the start of a cascade of terminal-electron-accepting processes indicating that nitrate removal was probably a reductive transformation. Where the alkaline FL9 microcosms differ significantly from the neutral H4 tests is that the aqueous sulphate concentration increased in all the microcosms except the sterile control. In the sterile control the sulphate concentration after autoclaving was initially higher than the other microcosms but remained steady throughout the test period. The increase in sulphate concentration was greatest in active microcosms (which all behaved similarly), and least in the chromate-only microcosm. The final concentration and general pattern of behaviour are compatible with desorption or dissolution of the solid phase sulphate found in the FL9 soil into the brook water, which would have occurred rapidly during autoclaving in the sterile control. Differences in final concentration are probably indicative of variability in the sulphate

concentration of the FL9 soil. Thus, in the alkaline microcosms, there is no indication of a cascade of stable-element terminal-electron-accepting processes had developed to the point of sulphate reduction.

In all three microbially active FL9 microcosms chromate removal started after nitrate removal was substantially complete, but before appreciable iron reduction was apparent, which suggests that Cr(VI) reduction was a direct enzymatic process as part of a cascade of terminal electron accepting processes. Microbial community analysis at the end of FL9c, where chromate removal was nearing completion indicates that species closely related to members of the Comamonadaceae family of β-proteobacteria dominated the population. Genera in the Comamonadaceae family and neighbouring phylogenetic groups are phenotypically highly diverse, even if they are phylogenetically closely related (Spring et al. 2005). However the sequences analysed had greatest similarity to members of the Acidovorax genus, most of which are capable of nitrate reduction (Straub et al. 2004; Willems et al. 1990).

The mineralogy of the two soil specimens was similar, with the small differences probably arising out of greater exposure of the FL9 specimen to highly alkaline COPR leachate; i.e higher calcite content, and greater sulphate concentration. It is probably the calcite precipitated during expose to COPR leachate that is responsible for buffering the FL9 microcosm pH to ~9.5. This pH difference would also be expected to influence the initial microbial populations of the two samples. In the neural H4 microcosms iron reduction followed nitrate removal more quickly, and occurred rapidly and completely, and was itself followed quite closely by sulphate removal. In the alkaline FL9 microcosms there was a lag period after nitrate removal (which occurred at similar rate in the neutral and alkaline

microcosms) before iron reduction was detectable, and then the rate and extent was quite variable between the FL9 microcosms but in all cases slower and less extensive than at neutral pH.

Cr(VI) reduction is far more rapid in the near neutral microcosms than in the alkaline ones. In the former case chromate reduction, like nitrate reduction, started within the first 48 hours, and an equimolar amount of each (~150 $\mu mol.l^{-1}$) was removed in the first 4 days. The nitrate was exhausted at that point, and the remainder of the chromate (~100 $\mu mol.l^{-1}$) was removed as iron reduction became established. In the alkaline FL9 microcosms chromate reduction did not appear to start until nitrate removal was complete. There was then a period when Cr(VI) was removed from solution with very little change in the amount of the total iron in the lower oxidation until some time after chromate removal started. The results from both H4 and FL9 microcosms are consistent with a cascade of terminal electron accepting process in redox potential order as show in Table 1 with chromate-reduction occurring between nitrate-reduction and iron-reduction. The redox potentials shown in Table 1 can be used to calculate the potential free energy yield per mole of acetate consumed at pH 7 and pH 9. The free energy yield of nitrate reduction barely changes (from -776 $kJ.mol^{-1}$ to -769 $kJ.mol^{-1}$) when the pH increases from 7 to 9, and hence it is not surprising that nitrate-reduction occurs rapidly in both neutral and high pH systems. Chromate- reduction (-537 $kJ.mol^{-1}$to -397 $kJ.mol^{-1}$), iron- reduction (-236 kJ mol^{-1} to -64 kJ mol^{-1}) and sulphate-reduction (-58 $kJ.mol^{-1}$ to -46 $kJ.mol^{-1}$), however, all show a reduction in free energy yield between pH 7 and 9. This decrease in free energy yield at higher pH, in combination with a less diverse microbial population, may help to explain why terminal electron accepting processes beyond nitrate reduction occur less vigorously in FL9 microcosms when compared to H4 microcosms.

This study has clearly shown that microbially mediated chromate reduction can be stimulated in both neutral and alkaline soil-water systems by addition of acetate. However, if this is to be the basis of a remedial treatment for contaminated sites, it is important that the chromium is not readily remobilised. It is reported that re-oxidation of Cr(III) by dissolved O_2 is kinetically inhibited in the near surface environment (van de Weijden and Reith 1982), and that the only important chemical oxidation pathway in natural systems is by Mn(IV)-oxides which is restricted by very low solubility of Cr(III) at neutral and high pH (Fendorf 1995; Fendorf and Zasoski 1992; Geelhoed et al. 2002). Thus, it appears that the stimulation of microbially mediated chromate reduction by addition of an electron donor has the potential to be a successful long-term treatment for soils affected by COPR contaminated sites

CONCLUSIONS

The addition of acetate to soil-water systems representative of soils contaminated by leachate from chromium ore processing residue resulted in chromate being removed from solution. Cr(VI) removal was consistent with a cascade of terminal electron accepting processes in soils, with Cr(VI) removal occurring between nitrate reduction and iron reduction. Removal only occurred in systems when microbially induced anoxia developed, indicating a microbially mediated process probably involving the reduction of the chromate to an insoluble Cr(III) species. At pH 7.7 Cr(VI) reduction started when there was still a significant rate of nitrate reduction, whereas at pH 9.3 Cr(VI) reduction occurred after nitrate-reduction was substantially complete but before there was clear evidence that iron-reduction had started. Thus microbially mediated Cr(VI) reduction is not dependant on establishing iron-reducing conditions, and may have been a direct enzymatic process. In both systems the microbial populations showed a significant increase in species closely related to β-proteobacteria capable of nitrate reduction at the point when Cr(VI) reduction was essentially

complete. Nitrate reduction occurred at a similar rate in the two soil-water systems, but Cr(VI) reduction and iron reduction were slower in the more alkaline system. This partial inhibition of terminal electron accepting processes in alkaline systems means that further work is needed to understand the process at high pH before biostimulation would be a viable treatment technology for COPR waste leachate affected soils.

ACKNOWLEDGEMENTS

This work was partially funded by a 2005/R2 Royal Society Research Grant. The authors would like to thank Dr Alison Baker, Reader in the Faculty of Biological Sciences, University of Leeds, and all the members of her research group for their invaluable advice and assistance with the molecular biology work reported in this paper. The first author would also like to thank Dr Julia Bailey-Serres, Professor of Genetics, Department of Botany and Plant Sciences, University of California Riverside, and all the members of her research group for generously giving their time and resources to teach him the basics of molecular biology.

REFERENCES

Anderson RT, Vrionis HA, Ortiz-Bernad I, Resch CT, Long PE, Dayvault R, Karp K, Marutzky S, Metzler DR, Peacock A and others. 2003. Stimulating the in-situ activity of Geobacter species to remove uranium from the groundwater of a uranium-contaminated aquifer. Applied and Environmental Microbiology 69(10):5884-5891.

Bader JL, Gonzalez G, Goodell PC, Ali AS, Pillai SD. 1999. Chromium-resistant bacterial populations from a site heavily contaminated with hexavalent chromium. Water Air and Soil Pollution 109(1-4):263-276.

Breeze VG. 1973. Land Reclamation and River Pollution Problems in Croal Valley Caused by Waste from Chromate Manufacture. Journal of Applied Ecology 10(2):513-525.

Burke IT, Boothman C, Lloyd JR, Livens FR, Charnock JM, McBeth JM, Mortimer RJG, Morris K. 2006. Reoxidation behavior of technetium, iron, and sulfur in estuarine sediments. Environmental Science & Technology 40(11):3529-3535.

Burke IT, Boothman C, Lloyd JR, Mortimer RJG, Livens FR, Morris K. 2005. Effects of Progressive Anoxia on the Solubility of Technetium in Sediments. Environmental Science & Technology 39(11): 4109-4116.

Cervantes C, Campos-Garcia J, Devars S, Gutierrez-Corona F, Loza-Tavera H, Torres-Guzman JC, Moreno-Sanchez R. 2001. Interactions of chromium with microorganisms and plants. FEMS Microbiology Reviews 25(3):335.

Chen JM, Hao OJ. 1998. Microbial chromium (VI) reduction. Critical Reviews in Environmental Science and Technology 28(3):219-251.

Darrie G. 2001. Commercial Extraction Technology and Process Waste Disposal in the Manufacture of Chromium chemicals From Ore. Environmental Geochemistry and Health 23(3):187-193.

Daulton TL, Little BJ, Jones-Meehan J, Blom DA, Allard LF. 2007. Microbial reduction of chromium from the hexavalent to divalent state. Geochimica et Cosmochimica Acta 71(3):556-565.

Deakin D. 2002. PhD Dissertation [PhD]: University of Leeds.

Deakin D, West LJ, Stewart DI, Yardley BWD. 2001. Leaching behaviour of a chromium smelter waste heap. Waste Management 21:265-270.
Donmez G, Kocberber N. 2005. Bioaccumulation of hexavalent chromium by enriched microbial cultures obtained from molasses and NaCl containing media. Process Biochemistry 40(7):2493-2498.
Eden PE, Schmidt TM, Blakemore RP, Pace NR. 1991. Phylogenetic analysis of Aquaspirillum magnetotacticum using polymerase chain reaction-amplified 16S rRNA-specific DNA. International Journal Systematic Bacteriology 41:324-325.
Farmer JG, Graham MC, Thomas RP, Licona-Manzur C, Licona-Manzur C, Paterson E, Campbell CD, Geelhoed JS, Lumsdon DG, Meeussen JCL and others. 1999. Assessment and Modelling of the Environmental Chemistry and Potential for Remediative Treatment of Chromium-Contaminated Land. Environmental Geochemistry and Health 21(4):331.
Fendorf SE. 1995. Surface-Reactions of Chromium in Soils and Waters. Geoderma 67(1-2):55-71.
Fendorf SE, Zasoski RJ. 1992. Chromium(III) oxidation by δ-MnO_2: 1. Characterization. Environmental Science & Technology 26(1):79-85.
Fude L, Harris B, Urrutia MM, Beveridge TJ. 1994. Reduction Of Cr(VI) By A Consortium Of Sulfate-Reducing Bacteria (SRB-III). Applied And Environmental Microbiology 60(5):1525-1531.
Geelhoed JS, Meeussen JCL, Hillier S, Lumsdon DG, Thomas RP, Farmer JG, Paterson E. 2002. Identification and geochemical modeling of processes controlling leaching of Cr(VI) and other major elements from chromite ore processing residue. Geochimica Et Cosmochimica Acta 66(22):3927-3942.
Geelhoed JS, Meeussen JCL, Roe MJ, Hillier S, Thomas RP, Farmer JG, Paterson E. 2003. Chromium remediation or release? Effect of iron(II) sulfate addition on chromium(VI) leaching from columns of chromite ore processing residue. Environmental Science & Technology 37(14):3206-3213.
Gemmell RP. 1973. Revegetation Of Derelict Land Polluted By A Chromate Smelter.1. Chemical Factors Causing Substrate Toxicity In Chromate Smelter Waste. Environmental Pollution 5:181-195.
Guertin J, Jacobs JA, Avakian CP, editors. 2005. Chromium(VI) Handbook. Boca Raton: CRC Press. 784 p.
Holmes DE, Finneran KT, O'Neil RA, Lovley DR. 2002. Enrichment of members of the family Geobacteraceae associated with stimulation of dissimilatory metal reduction in uranium- contaminated aquifer sediments. Applied and Environmental Microbiology 68(5):2300-2306.
Lane DL, Pace B, Olsen GJ, Stahl D, Sogin ML, R. PN. 1985. Rapid determination of 16S ribosomal RNA sequences for phylogenetic analysis. Proceedings of the National Academy of Science, USA. 82:6955-6959.
Langmuir D. 1997. Aqueous Environmental Geochemistry: Prentice-Hall.
Lloyd JR, Macaskie LE. 1996. A novel PhosphorImager-based technique for monitoring the microbial reduction of technetium. Applied and Environmental Microbiology 62(2):578-582.
Lloyd JR, Nolting HF, Sole VA, Bosecker K, Macaskie LE. 1998. Technetium reduction and precipitation by sulfate-reducing bacteria. Geomicrobiology Journal 15(1):45-58.
Lovley DR. 1993. Dissimilatory Metal Reduction. Annual Review of Microbiology 47:263-290.
Lovley DR, Phillips EJP. 1986. Availability of ferric iron for microbial reduction in bottom sediments of the freshwater tidal Potomac River. Appl. Environ. Microbiol. 52(2):751-757.
Lovley DR, Phillips EJP, Lonergan DJ, Widman PK. 1995. Fe(Iii) And S-0 Reduction By Pelobacter-Carbinolicus. Applied And Environmental Microbiology 61(6):2132-2138.
Martinez-Romero E. 2003. Diversity of Rhizobium-Phaseolus vulgaris symbiosis: overview and perspectives. Plant And Soil 252(1):11-23.
Moser DP, Fredrickson JK, Geist DR, Arntzen EV, Peacock AD, Li SMW, Spadoni T, McKinley JP. 2003. Biogeochemical processes and microbial characteristics across groundwater-surface water boundaries of the Hanford Reach of the Columbia River. Environmental Science & Technology 37(22):5127-5134.
NABIR. 2003. Bioremediation of metals and radionuclides: what it is and how it works. NABIR primer prepared for US Department of Energy. Report nr LBNL - 42595 (2003). p.78 p.
Neal AL, Lowe K, Daulton TL, Jones-Meehan J, Little BJ. 2002. Oxidation state of chromium associated with cell surfaces of Shewanella oneidensis during chromate reduction. Applied Surface Science 202(3-4):150.
Probian C, Wulfing A, Harder J. 2003. Anaerobic mineralization of quaternary carbon atoms: Isolation of denitrifying bacteria on pivalic acid (2,2-dimethylpropionic acid). Applied And Environmental Microbiology 69(3):1866-1870.
Richard FC, Bourg ACM. 1991. Aqueous geochemistry of chromium: A review. Water Research 25(7):807.
Scherer MM, Richter S, Valentine RL, Alvarez PJJ. 2000. Chemistry and microbiology of permeable reactive barriers for in situ groundwater clean up. Critical Reviews in Environmental Science and Technology 30:363 - 411.
Schmieman EA, Yonge DR, Petersen JN, Rege MA, Apel WA. 2000. Kinetics of chromium reduction by mixed cultures during growth phase. Water Environment Research 72(5):523-529.

Smith RL, Buckwalter SP, Repert DA, Miller DN. 2005. Small-scale, hydrogen-oxidizing-denitrifying bioreactor for treatment of nitrate-contaminated drinking water. Water Research 39(10):2014.
Spring S, Wagner M, Schumann P, Kampfer P. 2005. Malikia granosa gen. nov., sp. nov., a novel polyhydroxyalkanoate- and polyphosphate-accumulating bacterium isolated from activated sludge, and reclassification of Pseudomonas spinosa as Malikia spinosa comb. nov. Int J Syst Evol Microbiol 55(2):621-629.
Straub KL, Schonhuber WA, Buchholz-Cleven BEE, Schink B. 2004. Diversity of ferrous iron-oxidizing, nitrate-reducing bacteria and their involvement in oxygen-independent iron cycling. Geomicrobiology Journal 21(6):371-378.
Stumm W, Morgan JJ. 1996. Aquatic Geochemistry. New York: John Wiley and Sons.
Suzuki T, Miyata N, Horitsu H, Kawai K, Takamizawa K, Tai Y, Okazaki M. 1992. NAD(P)H-dependent chromium (VI) reductase of Pseudomonas ambigua G-1: a Cr(V) intermediate is formed during the reduction of Cr(VI) to Cr(III). J. Bacteriol. 174(16):5340-5345.
Thauer RK, Jungermann K, Decker K. 1977. Energy conservation in chemotrophic anaerobic bacteria. Bacteriological Reviews 41(1):100-180.
US-EPA. 1992. SW-846 Manual: Method 7196a. Chromium hexavalent (colorimetric). US EPA.
van de Weijden CH, Reith M. 1982. Chromium (III) - chromium (VI) interconversions in seawater. Marine Chemistry 11:565-572.
Viamajala S, Peyton BM, Apel WA, Petersen JN. 2002a. Chromate reduction in Shewanella oneidensis MR-1 is an inducible process associated with anaerobic growth. Biotechnology Progress 18(2):290-295.
Viamajala S, Peyton BM, Apel WA, Petersen JN. 2002b. Chromate/nitrite interactions in Shewanella oneidensis MR-1: Evidence for multiple hexavalent chromium Cr(VI) reduction mechanisms dependent on physiological growth conditions. Biotechnology and Bioengineering 78(7):770-778.
Viamajala S, Peyton BM, Sani RK, Apel WA, Petersen JN. 2004. Toxic effects of chromium(VI) on anaerobic and aerobic growth of Shewanella oneidensis MR-1. Biotechnology Progress 20(1):87-95.
Viollier E, Inglett PW, Hunter K, Roychoudhury P, Van Cappellen P. 2000. The ferrozine method revisited: Fe(II)/Fe(III) determination in natural waters. Appl. Geochem. 15:785-790.
Willems A. 2006. The taxonomy of rhizobia: an overview. Plant And Soil 287(1-2):3-14.
Willems A, Falsen E, Pot B, Jantzen E, Hoste B, Vandamme P, Gillis M, Kersters K, Deley J. 1990. Acidovorax, A New Genus For Pseudomonas-Facilis, Pseudomonas-Delafieldii, E-Falsen (Ef) Group 13, Ef Group 16, And Several Clinical Isolates, With The Species Acidovorax-Facilis Comb-Nov, Acidovorax-Delafieldii Comb-Nov, And Acidovorax-Temperans Sp-Nov. International Journal Of Systematic Bacteriology 40(4):384-398.
Ye Q, Roh Y, Carroll SL, Blair B, Zhou JZ, Zhang CL, Fields MW. 2004. Alkaline anaerobic respiration: Isolation and characterization of a novel alkaliphilic and metal-reducing bacterium. Applied and Environmental Microbiology 70(9):5595-5602.

Table 1: Microbially significant half-reaction reduction potentials: Standard Reduction Potential, E^0, and redox potential, Eh, at pH 7 and 9 (at 25°C and atmospheric pressure).

Transformation	**Reaction**	**E_0 (V)**	**Eh @ pH 7 (V)**	**Eh @ pH 9 (V)**	**Assumptions**
O_2 depletion [+]	$O_2 + 4H^+ + 4e^- = 2H_2O$	1.230	0.805	0.687	P_{O_2}=0.2 bar
Denitrification [+]	$NO_3^- + 6H^+ + 5e^- = ½N_2 + 3H_2O$	1.240	0.713	0.571	$[NO_3^-]$=1 mmols l^{-1} P_{N_2}=0.8 bar
Mn reduction [+] Mn(IV) to Mn(II)	$MnO_2 + 4H^+ + 2e^- = Mn^{2+} + 2H_2O$	1.230	0.544	0.308	$[Mn^{2+}]$=18 μmols l^{-1}
Fe reduction [+] Fe(III) to Fe(II)	$Fe(OH)_3 + 3H^+ + e^- = Fe^{2+} + 3H_2O$	0.975	0.014	-0.342	$[Fe^{2+}]$=18 μmols l^{-1}
Sulfate reduction [+] S(VI) to S(–II)	$SO_4^{2-} + 10H^+ + 8e^- = H_2S + 4H_2O$	0.301	–0.217	-0.365	$[SO_4^{2-}]=[H_2S]$
Methane generation [+] C(IV) to C(–IV)	$HCO_3^- + 9H^+ + 8e^- = CH_4 + 3H_2O$	0.206	–0.260	-0.393	$[HCO_3^-]=[CH_4]$
H_2 generation [+] H(I) to H(0)	$H^+ + e^- = ½H_2$	0.000	–0.414	-0.533	P_{H_2}=1 bar
Cr reduction * Cr(VI) to Cr(III)	$CrO_4^{2-} + 8H^+ + 3e^- = Cr^{3+} + 4H_2O$	1.507	0.404	0.089	$[CrO_4^{2-}]=[Cr^{3+}]$
Bicarbonate reduction to acetate [×] C(VI) to C(0)	$2HCO_3^- + 9H^+ + 8e^- = CH_3COO^- + 4H_2O$	0.187	-0.292	-0.425	$[HCO_3^-]=[CH^3COO^-]$ = 20 mmols l^{-1}

[+] after (Langmuir 1997)

* calculated using thermodynamic data from (Stumm and Morgan 1996)

[×] calculated using thermodynamic data from (Thauer et al. 1977)

Table 2: Pore water composition of COPR at the study site (Deakin 2002)

	Na^+	K^+	Ca^+	SO_4^{2-}	Cl^-	AlO_2^-	CrO_4^{2-}	CO_3^{2-}	pH
Concentration ($mmol.l^{-1}$)	10	0.6	10	6.2	0.7	0.1	0.6	0.3	12.3

Cations were measured by ICP-AES, anions were measured by Ion Chromatography on a Dionex DX-100, except for carbonate which was measured by the flow injection method.

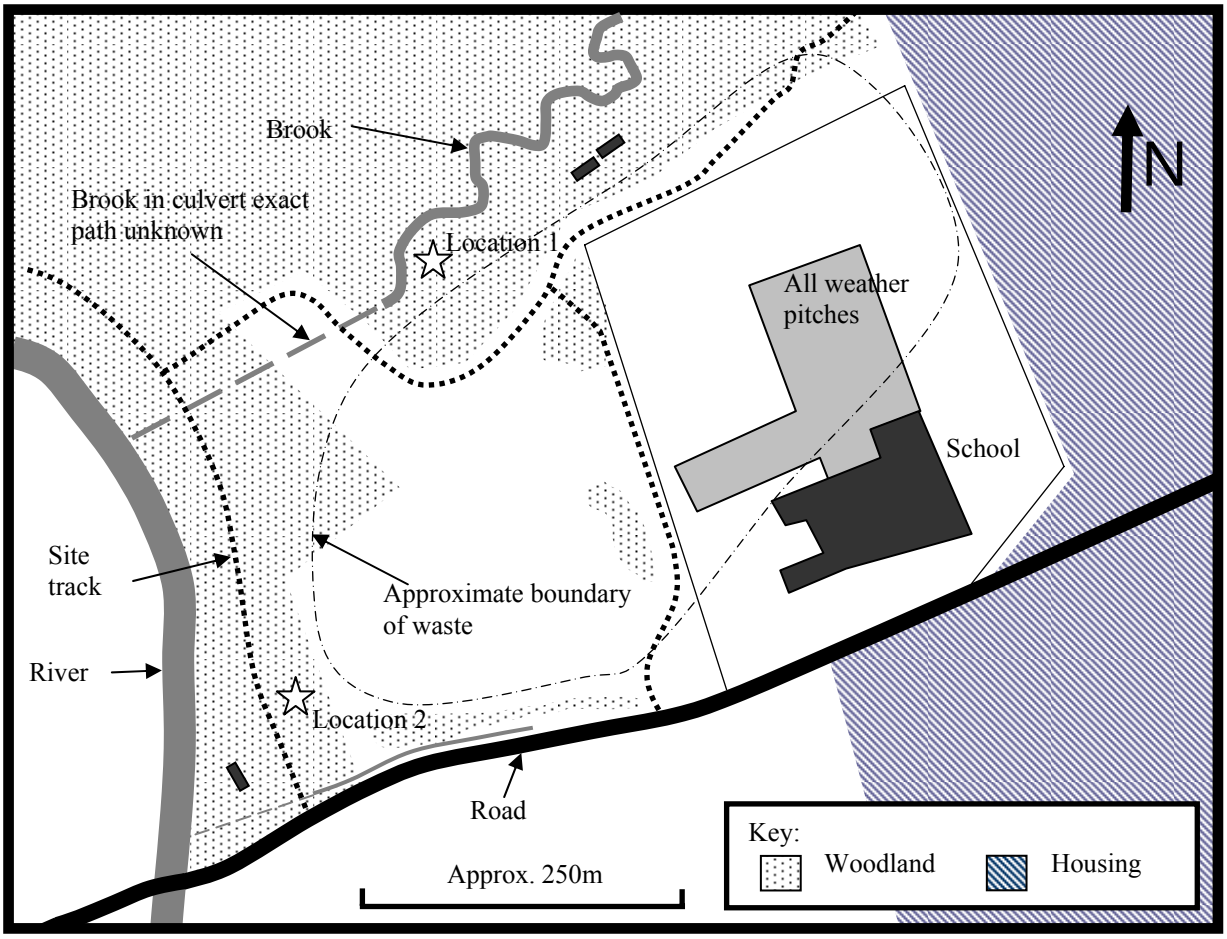

Figure 1: Sketch map of the site showing the sampling locations (redrawn from a Google Earth image of the site).

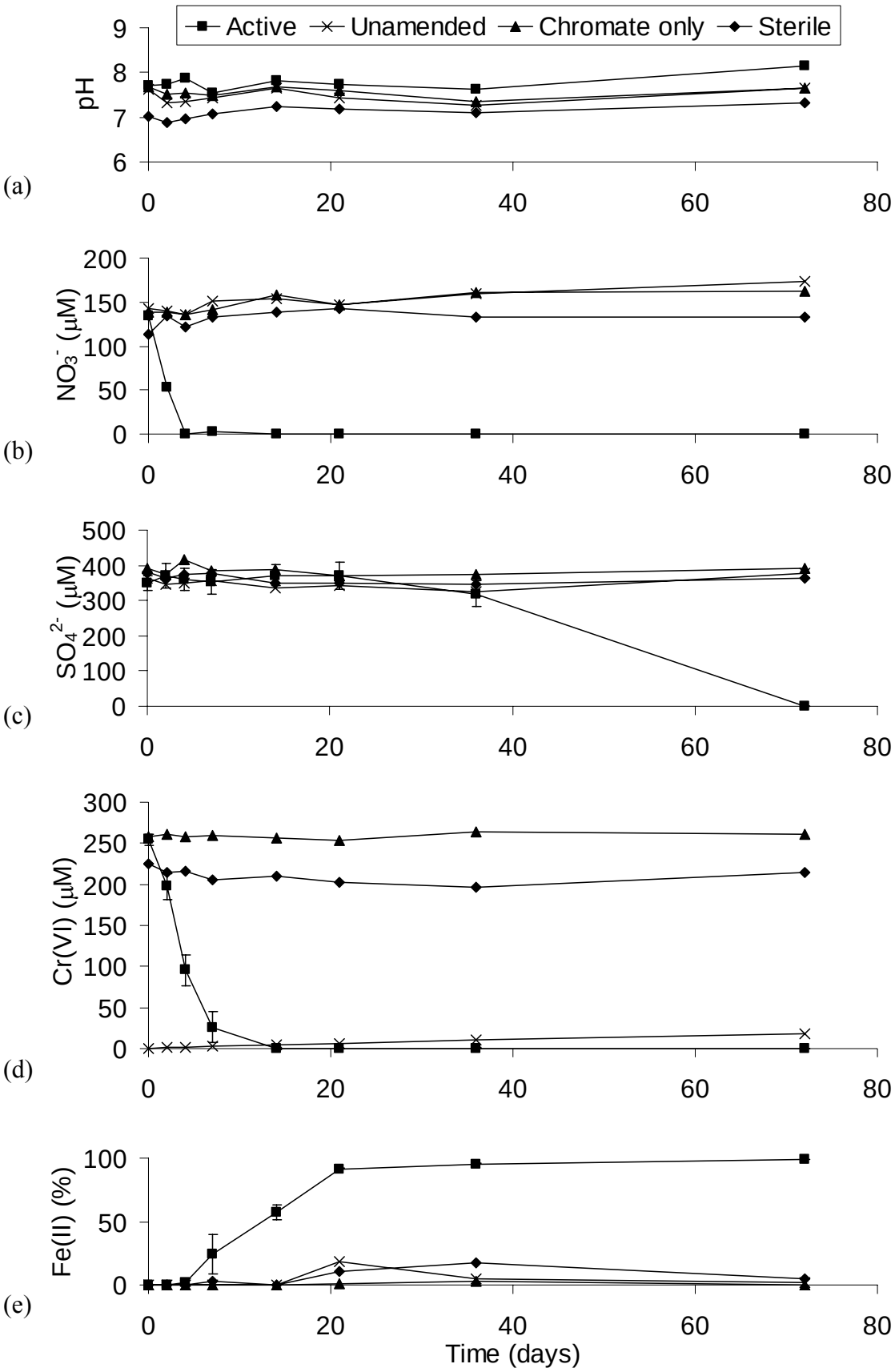

Figure 2: Geochemical response of the microcosms containing soil H4: (a) – (d) pH, nitrate, sulphate and Cr(VI) concentrations in the aqueous phase, and (e) speciation of iron extracted from solid phase (error bars of ±1 standard deviation are shown on average data from the microbially active microcosms).

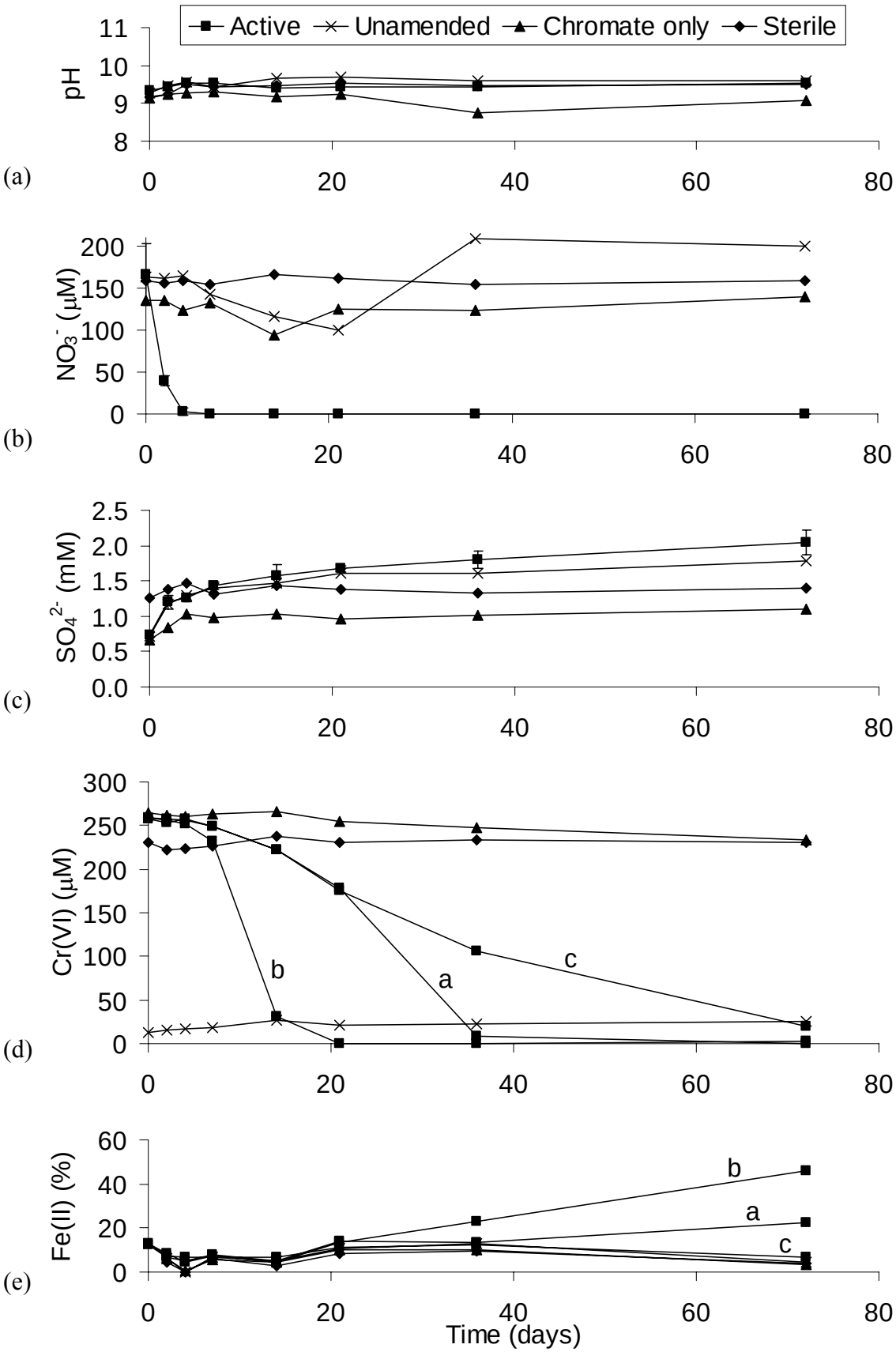

Figure 3: Geochemical response of the microcosms containing soil FL9: (a) – (d) pH, nitrate, sulphate and Cr(VI) concentrations in the aqueous phase, and (e) speciation of iron extracted from solid phase (data from microbially active microcosms a, b, and c are shown separately where appropriate, otherwise error bars of ±1 standard deviation are shown on average data).

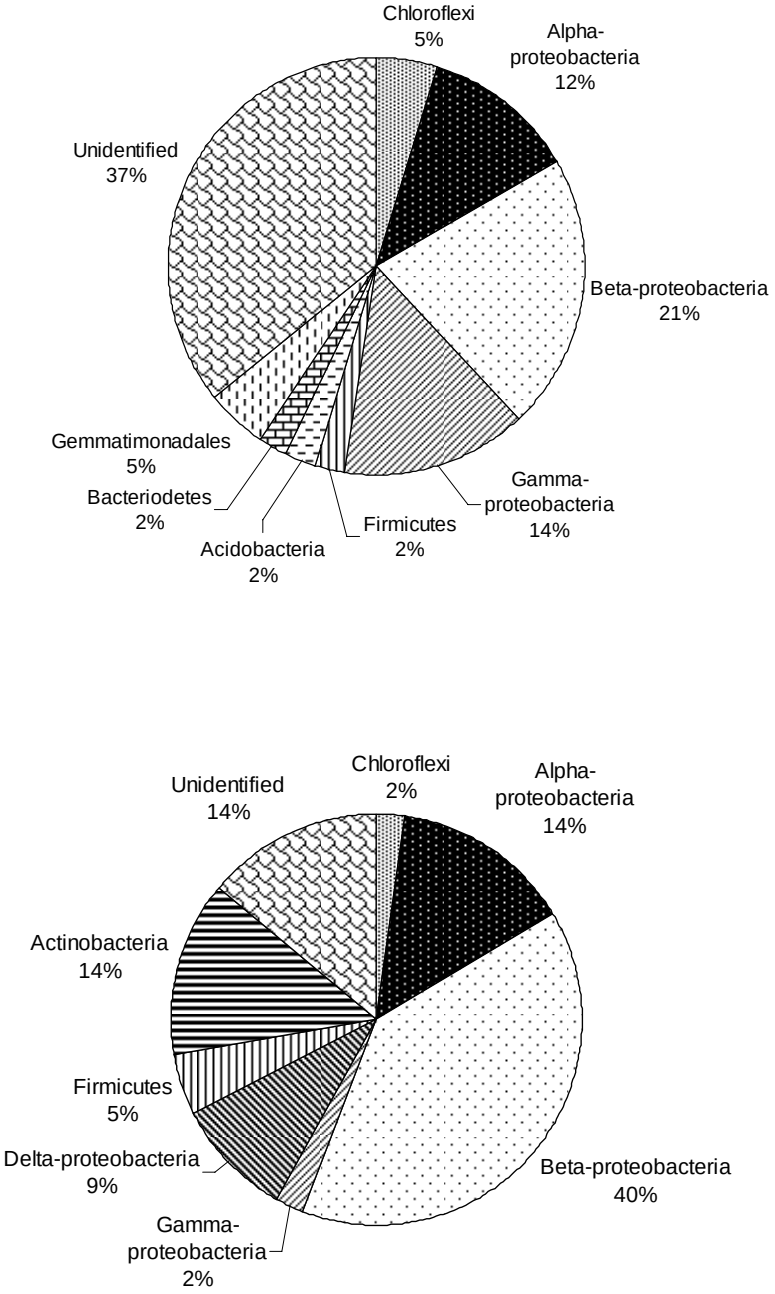

Figure 4. Shifts in the microbial community of the sample H4; untreated soil (top) (42 clones), and after incubation under anaerobic conditions with added acetate (bottom) (43 clones). Charts show phylogenetic affiliation of the 16S rRNA gene sequences.

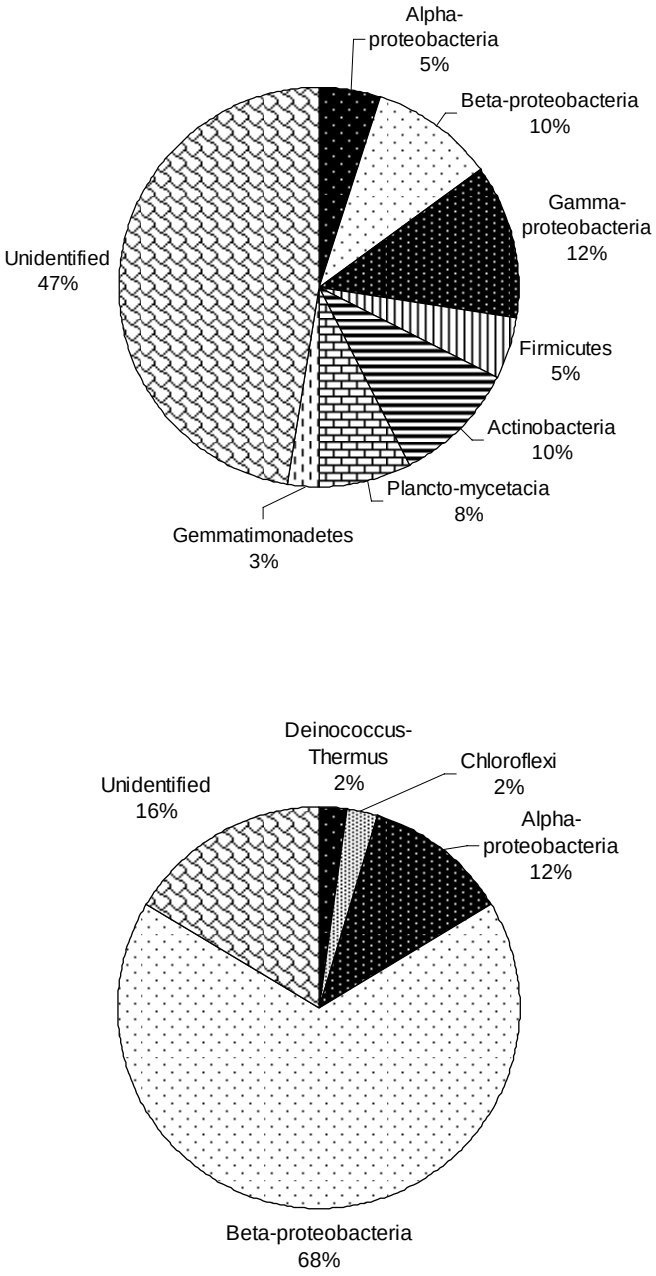

Figure 5. Shifts in the microbial community of the sample FL9; untreated soil (top) (40 clones), and after incubation under anaerobic conditions with added acetate (bottom) (43 clones). Charts show phylogenetic affiliation of the 16S rRNA gene sequences.

Appendix A

Table A.1. Clone table showing the Genebank accession number and phylogenetic affiliation of the 16S rDNA gene sequences

ID	Accession number	Closest identified microorganism (accession number)	Identity	% Match	E-Value*	Phylogenetic Division
H4 T_0-1	AM884621	Gamma proteobacterium clone (AY144261)	482/489	98	0	γ-proteobacteria
H4 T_0-2	AM884622	Acidobacterium clone (AY922096)	534/538	99	0	Acidobacteria
H4 T_0-4	AM884623	Beta proteobacterium clone (EU043637)	466/471	98	0	β-proteobacteria
H4 T_0-5	AM884624	Beta proteobacterium clone (AY921702)	513/521	98	0	β-proteobacteria
H4 T_0-7	AM884625	Comamonadaceae clone (EF018476)	507/522	97	0	β-proteobacteria
H4 T_0-9	AM884626	Xanthomonadaceae clone (DQ230964)	499/522	95	0	γ-proteobacteria
H4 T_0-11	AM884627	Gemmatimonadetes clone (EF555722)	449/454	98	0	Gemmatimonadetes
H4 T_0-13	AM884628	Hyphomicrobiaceae (EF019366)	468/473	98	0	α-proteobacteria
H4 T_0-15	AM884629	Alpha proteobacterium clone (AB252934)	431/446	96	0	α-proteobacteria
H4 T_0-16	AM884630	Beta Proteobacterium clone (AY948000)	465/477	97	0	β-proteobacteria
H4 T_0-18	AM884631	Beta Proteobacterium clone (AY435511)	500/521	95	0	β-proteobacteria
H4 T_0-19	AM884632	Green nonsulfur clone (AY043952)	433/452	95	0	Chloroflexi
H4 T_0-21	AM884633	Alpha proteobacterium clone (AB252934)	403/423	95	0	α-proteobacteria
H4 T_0-22	AM884634	Gemmatimonadetes clone (DQ828292)	463/476	97	0	Gemmatimonadetes
H4 T_0-23	AM884635	Bacteroidetes clone (AM747101)	449/454	98	0	Bacteriodetes
H4 T_0-27	AM884636	Xanthomonadaceae clone (DQ230964)	416/433	96	0	γ-proteobacteria
H4 T_0-28	AM884637	Aquabacterium sp. (DQ167099)	487/496	98	0	β-proteobacteria
H4 T_0-32	AM884638	Firmicutes clone (EF651037)	400/420	95	0	Firmicutes
H4 T_0-34	AM884639	Hydrogenaphaga sp. (EF540470)	499/499	100	0	β-proteobacteria
H4 T_0-35	AM884640	Acidovorax sp. (DQ128112)	457/461	99	0	β-proteobacteria
H4 T_0-36	AM884641	Alpha proteobacteria (AB252934)	430/445	96	0	α-proteobacteria
H4 T_0-37	AM884642	Psuedomonas sp (AY880304)	493/496	99	0	γ-proteobacteria
H4 T_0-38	AM884643	Rhodocyclaceae clone (EF018601)	484/494	97	0	β-proteobacteria
H4 T_0-39	AM884644	Hyphomicrobiaceae clone (EF020212)	456/471	96	0	α-proteobacteria
H4 T_0-b	AM884645	Green nonsulfur clone (AY043952)	435/455	95	0	Chloroflexi
H4 T_0-d	AM884646	Xanthomonadales sp. (EF664375)	457/457	100	0	γ-proteobacteria
H4 T_0-e	AM884647	Xanthomonas sp. (DQ128122)	483/501	96	0	γ-proteobacteria
H4aT_{14}-1	AM884648	Hyphomicrobiaceae clone (EF019849)	460/473	97	0	α-proteobacteria
H4aT_{14}-2	AM884649	Rhodocyclus sp. (AY691423)	505/523	96	0	β-proteobacteria
H4aT_{14}-3	AM884650	Rhizobium giardinii (U86344)	458/470	97	0	α-proteobacteria
H4aT_{14}-4	AM884651	Comamonadaceae sp. (AJ505857)	486/487	99	0	β-proteobacteria
H4aT_{14}-5	AM884652	Rhodoferax ferrireducens (CP000267)	516/524	98	0	β-proteobacteria
H4aT_{14}-8	AM884653	Rhodocyclus sp. (AY691423)	503/523	96	0	β-proteobacteria
H4aT_{14}-9	AM884654	Hydrogenophaga sp. (AB166889)	476/499	95	0	β-proteobacteria
H4aT_{14}-11	AM884655	Rhodocyclus sp. (AY691423)	483/501	96	0	β-proteobacteria
H4aT_{14}-12	AM884656	Comamonadaceae sp. (AJ505858)	494/499	98	0	β-proteobacteria
H4aT_{14}-13	AM884657	Arthrobacter sp. (DQ157989)	482/482	100	0	Actinobacteria
H4aT_{14}-15	AM884658	Fusibacter sp. (AF491333)	485/510	95	0	Firmicutes
H4aT_{14}-16	AM884659	Arthrobacter sp. (EF540513)	476/478	99	0	Actinobacteria
H4aT_{14}-17	AM884660	Actinobacterium sp. (AB265917)	460/482	95	0	Actinobacteria
H4aT_{14}-20	AM884661	Actinobacterium clone (EF219697)	487/500	97	0	Actinobacteria

ID	Accession number	Closest identified microorganism (accession number)	Identity	% Match	E-Value*	Phylogenetic Division
H4aT$_{14}$-21	AM884662	Aquaspirillum metamorphum (Y18618)	474/494	95	0	β-proteobacteria
H4aT$_{14}$-22	AM884663	Propionivibrio sp. (AY643079)	483/501	96	0	β-proteobacteria
H4aT$_{14}$-24	AM884664	Pseudomonas sp (DQ985230)	515/521	98	0	γ-proteobacteria
H4aT$_{14}$-25	AM884665	Geobacteraceae clone (EF668930)	531/540	98	0	δ-proteobacteria
H4aT$_{14}$-26	AM884666	Chloroflexi clone (AY922044)	471/492	95	0	Chloroflexi
H4aT$_{14}$-27	AM884667	Comamonadaceae sp. (AJ505857)	507/511	99	0	β-proteobacteria
H4aT$_{14}$-28	AM884668	Rhodocyclus sp. (AY691423)	508/525	96	0	β-proteobacteria
H4aT$_{14}$-29	AM884669	Geobacteraceae clone (EF059536)	507/517	98	0	δ-proteobacteria
H4aT$_{14}$-30	AM884670	Rhodocyclus sp. (AY691423)	500/525	95	0	β-proteobacteria
H4aT$_{14}$-31	AM884671	Rhizobium sp. (AF345554)	462/470	98	0	α-proteobacteria
H4aT$_{14}$-32	AM884672	Rhizobium sp. (AF345554)	467/470	99	0	α-proteobacteria
H4aT$_{14}$-33	AM884673	Actinobacterium clone (AB265835)	438/460	95	0	Actinobacteria
H4aT$_{14}$-34	AM884674	Rhodocyclus sp. (AY691423)	507/523	96	0	β-proteobacteria
H4aT$_{14}$-35	AM884675	Hyphomicrobiaceae clone (EF018692)	448/471	95	0	α-proteobacteria
H4aT$_{14}$-36	AM884676	Geobacteraceae clone (EF668930)	509/515	98	0	δ-proteobacteria
H4aT$_{14}$-39	AM884677	Rhodocyclus sp. (AY691423)	502/520	96	0	β-proteobacteria
H4aT$_{14}$-40	AM884678	Rhodocyclus sp. (AY691423)	509/525	96	0	β-proteobacteria
H4aT$_{14}$-41	AM884679	Rhizobium sp. (DQ096643)	464/469	98	0	α-proteobacteria
H4aT$_{14}$-42	AM884680	Comamonadaceae clone (DQ628936)	496/501	99	0	β-proteobacteria
H4aT$_{14}$-43	AM884681	Arthrobacter sp. (DQ157989)	505/506	99	0	Actinobacteria
H4aT$_{14}$-45	AM884682	Clostridium puniceum (X71857)	465/472	98	0	Firmicutes
H4aT$_{14}$-46	AM884683	Methylibium petroleiphilum (CP000555)	504/521	96	0	β-proteobacteria
H4aT$_{14}$-48	AM884684	Geobacteraceae clone (EF668930)	524/538	97	0	δ-proteobacteria
FL9 T$_0$-5	AM884685	Gamma proteobacterium (DQ507153)	508/525	96	0	γ-proteobacteria
FL9 T$_0$-6	AM884686	Arthrobacter luteolus (AJ243422)	480/489	98	0	Actinobacteria
FL9 T$_0$-9	AM884687	Nitrosospira sp. (X90820)	479/499	95	0	β-proteobacteria
FL9 T$_0$-10	AM884688	Gamma proteobacterium (F072052)	480/493	97	0	γ-proteobacteria
FL9 T$_0$-11	AM884689	Planctomycete (BX294900)	407/419	97	0	Planctomycetes
FL9 T$_0$-14	AM884690	Gamma proteobacterium (AY632508)	474/487	97	0	γ-proteobacteria
FL9 T$_0$-15	AM884691	Nitrosospira sp. (X90820)	501/523	95	0	β-proteobacteria
FL9 T$_0$-20	AM884692	Acidovorax sp. (DQ133409)	480/486	98	0	β-proteobacteria
FL9 T$_0$-21	AM884693	Micromonospora peucetia (X92603)	467/474	98	0	Actinobacteria
FL9 T$_0$-22	AM884694	Planctomycete clone (AY922083)	486/477	98	0	Planctomycetes
FL9 T$_0$-25	AM884695	Xanthomonas sp. (DQ128122)	484/500	96	0	γ-proteobacteria
FL9 T$_0$-X3	AM884696	Beta proteobacteria sp. (AJ853867)	492/496	99	0	β-proteobacteria
FL9 T$_0$-X4	AM884697	Xanthomonas sp. (DQ128122)	484/503	96	0	γ-proteobacteria
FL9 T$_0$-X5	AM884698	Clostridium gasigenes (AF092548)	475/492	96	0	Firmicutes
FL9 T$_0$-X7	AM884699	Micromonospora sp. (EF212015)	487/500	97	0	Actinobacteria
FL9 T$_0$-X8	AM884700	Planctomycete sp. (AY921993)	486/499	97	0	Planctomycetes
FL9 T$_0$-X9	AM884701	Gemmatimonadetes sp. (DQ828292)	479/502	95	0	Gemmatimonadetes
FL9 T$_0$-X13	AM884702	Endosymbiont of Acanthmoeba sp. (EF140634)	461/485	95	0	α-proteobacteria
FL9 T$_0$-X15	AM884703	Alpha proteobacteria sp. (AF445680)	446/465	95	0	α-proteobacteria
FL9 T$_0$-X17	AM884704	Micromonospora pattaloongensis (AB275607)	489/498	98	0	Actinobacteria
FL9 T$_0$-X24	AM884705	Clostridium gasigenes (AF092548)	476/494	96	0	Firmicutes

ID	Accession number	Closest identified microorganism (accession number)	Identity	% Match	E-Value*	Phylogenetic Division
FL9cT$_{72}$-1	AM884706	Rhodobacter gluconium (DQ363135)	446/468	95	0	α-proteobacteria
FL9cT$_{72}$-2	AM884707	Deinococcus sp. (DQ128152)	460/472	97	0	Deinococcus-Thermus
FL9cT$_{72}$-3	AM884708	Burkholderiales clone (EF667920)	494/520	95	0	β-proteobacteria
FL9cT$_{72}$-4	AM884709	Rhodobacter gluconium (DQ363135)	447/468	95	0	α-proteobacteria
FL9cT$_{72}$-5	AM884710	Acidovorax sp. (DQ133409)	481/484	99	0	β-proteobacteria
FL9cT$_{72}$-6	AM884711	Hydrogenophaga taeniospiralis (AY771764)	492/505	97	0	β-proteobacteria
FL9cT$_{72}$-7	AM884712	Hydrogenophaga atypica (AJ585992)	507/522	97	0	β-proteobacteria
FL9cT$_{72}$-9	AM884713	Chloroflexi sp. (AB265904)	453/472	95	0	Choroflexi
FL9cT$_{72}$-10	AM884714	Acidovorax sp. (DQ128112)	480/486	98	0	β-proteobacteria
FL9cT$_{72}$-11	AM884715	Comamonadaceae sp. (AJ505857)	511/514	99	0	β-proteobacteria
FL9cT$_{72}$-12	AM884716	Acidovorax sp. (DQ133409)	480/484	99	0	β-proteobacteria
FL9cT$_{72}$-13	AM884717	Acidovorax sp. (DQ128112 and DQ133409)	482/484	99	0	β-proteobacteria
FL9cT$_{72}$-14	AM884718	Acidovorax sp. (DQ128112 and DQ133409)	484/486	99	0	β-proteobacteria
FL9cT$_{72}$-15	AM884719	Acidovorax sp. (DQ128112 and DQ133409)	476/484	98	0	β-proteobacteria
FL9cT$_{72}$-16	AM884720	Acidovorax sp. (DQ128112 and DQ133409)	482/484	99	0	β-proteobacteria
FL9cT$_{72}$-18	AM884721	Burkholderiales clone (EF667920)	495/520	95	0	β-proteobacteria
FL9cT$_{72}$-24	AM884722	Acidovorax sp. (DQ128112 and DQ133409)	481/484	99	0	β-proteobacteria
FL9cT$_{72}$-25	AM884723	Hyphomicrobiaceae sp. (EF073503)	412/420	98	0	α-proteobacteria
FL9cT$_{72}$-26	AM884724	Acidovorax sp. (DQ128112)	477/486	98	0	β-proteobacteria
FL9cT$_{72}$-27	AM884725	Acidovorax sp. (DQ128112)	484/486	99	0	β-proteobacteria
FL9cT$_{72}$-28	AM884726	Hyphomicrobiaceae sp. (EF019706)	468/473	98	0	α-proteobacteria
FL9cT$_{72}$-29	AM884727	Acidovorax sp. (DQ128112 and DQ133409)	482/484	99	0	β-proteobacteria
FL9cT$_{72}$-30	AM884728	Acidovorax sp. (DQ128112)	469/484	96	0	β-proteobacteria
FL9cT$_{72}$-31	AM884729	Comamonadaceae sp. (AJ505858)	488/491	99	0	β-proteobacteria
FL9cT$_{72}$-32	AM884730	Acidovorax sp. (DQ128112)	485/486	99	0	β-proteobacteria
FL9cT$_{72}$-33	AM884731	Acidovorax sp. (DQ128112 and DQ133409)	464/465	99	0	β-proteobacteria
FL9cT$_{72}$-34	AM884732	Acidovorax sp. (DQ128112 and DQ133409)	484/486	99	0	β-proteobacteria
FL9cT$_{72}$-35	AM884733	Acidovorax sp. (DQ128112 and DQ133409)	450/457	98	0	β-proteobacteria
FL9cT$_{72}$-36	AM884734	Acidovorax sp. (DQ128112 and DQ133409)	485/486	99	0	β-proteobacteria
FL9cT$_{72}$-37	AM884735	Acidovorax sp. (DQ128112 and DQ133409)	482/484	99	0	β-proteobacteria
FL9cT$_{72}$-38	AM884736	Acidovorax sp. (DQ128112)	463/463	100	0	β-proteobacteria
FL9cT$_{72}$-39	AM884737	Acidovorax sp. (DQ128112 and DQ133409)	485/486	99	0	β-proteobacteria
FL9cT$_{72}$-40	AM884738	Acidovorax sp. (DQ128112 and DQ133409)	482/484	99	0	β-proteobacteria
FL9cT$_{72}$-43	AM884739	Acidovorax sp. (DQ128112 and DQ133409)	485/486	99	0	β-proteobacteria
FL9cT$_{72}$-45	AM884740	Alpha proteobacterium sp. (DQ211366)	452/466	96	0	α-proteobacteria
FL9cT$_{72}$-46	AM884741	Acidovorax sp. (DQ128112)	458/460	99	0	β-proteobacteria

* The BLAST E-value indicates the likelihood that a match has arisen by chance.